27th EPS Conference on Contr. Fusion and Plasma Phys. Budapest, 12-16 June 2000 ECA Vol. **24B** (2000) 1669 -1672

Development of an electron Bernstein emission diagnostic for temperature profiles above the ECE-cutoff density at Wendelstein 7-AS Stellarator

F.Volpe, H.P.Laqua and the W7-AS Team

Max-Planck-Institut für Plasmaphysik, EURATOM Association
D-85748 Garching, Germany

Abstract

A diagnostic based on the radiometry of thermal emission of electron Bernstein waves (EBW) is under development at W7-AS, to measure the electron temperature profile at densities higher than the ECE cutoff. It is based on mode conversions into e.m.waves, polarized firstly in extraordinary (X) mode and then in ordinary (O) mode (so called BXO process).
In order for the XO conversion to occur, the sightline has to be orientated at an oblique "optimal angle" with respect to the magnetic field and to the plasma cutoff layer, therefore the polarization of the detected O-mode is elliptical. A broadband polarizer ($f = 66 \div 76GHz$), a waveguide with elliptical cross-section, converts the polarization from elliptical to linear. The signal is then analysed by a single-side-band heterodyne radiometer. To convert the experimental spectra into temperature profiles, it is necessary to reconstruct the complicated mode-converted ray paths in the plasma. Spectral measurements and the first temperature profile are presented and discussed in terms of ray-tracing calculations in full stellarator geometry.

Motivation

Some magnetically confined plasmas may not fulfill the accessibility criteria for the fundamental O-mode, $\omega_{pe} < \omega_{ce}$, and eventually for the second harmonic of the X-mode, $\omega_{pe}^2 < \omega^2 - \omega\omega_{ce}$. This may hold in high density stellarator plasmas, not affected by the Greenwald limit, and in low magnetic field spherical tori. In such cases the electron Bernstein waves (EBW) become appealing for heating/diagnostic purposes since they propagate without density limit until/after they are cyclotron damped/emitted.
The heating potential of EBW was already demonstrated at W7-AS [1] taking advantage of the OXB scheme [3] proposed by Preinhaelter and Kopecký and based on mode conversions from O-mode to X-mode and finally to Bernstein waves (B).
At W7-AS the first measurements of emission have also been realized [2], employing the reversed scheme, BXO, and the aim is now to relate the mode-converted emission to the electron temperature profile.

Ray-tracing

The coupling of O and X-mode occurs at the cutoff layer for the O-mode. There, the two modes are degenerate if the beam crosses the layer with a special oblique orientation, such that $2(1+\frac{\omega_{ce}}{\omega})(k_{\|,opt}-k_{\|})^2+k_y^2=0$ [4], where $k_{\|}$ is the component of the wavevector parallel to the magnetic field $\mathbf{B}$, $k_{\|,opt}$ an optimal value given in [3] and k_y is the component perpendicular to both $\mathbf{B}$ and the density gradient. Because of the finite $k_{\|}$, the mode-

converted rays follow complicated paths in the plasma. Besides, in an inhomogeneous plasma $k_{||}$ itself generally evolves in a complicated way. Therefore it is necessary to trace the rays, to find where the Doppler broadened cyclotron resonance $\omega - k_{||}v_{th} - \frac{n\omega_{ce}}{\gamma} = 0$ (n=1 in our case) is met. For this purpose a ray-tracing code inclusive of mode conversions has been developed, extending the approach of ref.[5] from tokamak to full stellarator geometry. The determinant of the Hermitian part of the hot dielectric tensor is a sensitive function of **B**. As a consequence, the ray paths depend strongly on the poloidal component B_p, on the toroidal curvature of **B** (even in a large aspect-ratio device as W7-AS), on the tilt of the sightline relative to the equatorial plane (in agreement with [6]) and on the broken axisymmetry of **B** in the stellarator.

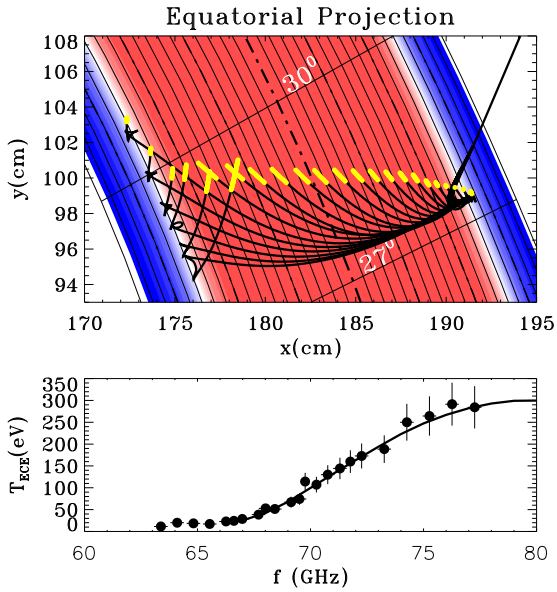

Figure 1: [top] EBWs ray tracing for $B = 2.4T$ and $n_e = 1.7 \cdot 10^{14} cm^{-3}$ at center, $f = 67 \div 90GHz$, step $1GHz$. Red is the overdense plasma core, yellow where the signals take origin; [bottom] Experimental (circles) and simulated (solid line) spectrum

The synergy of all these effects solves the disagreement formerly found between experiments and 2D simulations [2]. Detailed 3D calculations now agree with the experiments described in [2] and with new measurements performed along the same sightline, as fig.1 shows.

This sightline, starting at toroidal position $\varphi = 28^0$, unfortunately leads to large $k_{||}$ and therefore to large Doppler shift of the spectrum, $k_{||}v_{th} = 10 \div 20GHz$. Being temperature-dependent, this shift is of course unfavourable from the diagnostic point of view.

For this reason possible antenna positions and orientations have been scanned by means of ray-tracing. The best sightline (that with the lowest Doppler shift, $< 3GHz$, and the highest transmittivity at the cutoff, $> 90\%$) has been found in the neighbourhood of the tokamak-like section of the plasma, $\varphi = 36^0$, and is slightly tilted upwards as a consequence of finite B_p.

Experimental set-up

An antenna has been built, viewing the plasma along the best sightline with the focus at the XO conversion layer. The antenna consists of both an ellipsoidal and a plane mirror and of a corrugated horn. The millimeter wave signal is then carried by a circular waveguide, polarization-conserving, to a quarter wave phase shifter. In fact the polarization of the O-mode detected along the oblique sightline is elliptical, but by 90^0 phase shift and proper orientation of optical axes it can be changed into a linear one.

The device is required to cover the broad band $f = 66 \div 76GHz$ with a systematic error in the phase shift smaller than 20%, corresponding to 4% in intensity, which can be neglected in comparison with statistical errors of 10%, typical of ECE radiometry.

Three phase shifters have been compared: an array of metal plates, sometimes referred to as "artificial dielectric" [7], a non-uniformly grooved mirror [8] placed in the 60^0 miter bend of a polarization rotator (two 120^0 miter bends separated by a 60^0 one) and an

elliptical waveguide, whose principle can be summarized as follows. Going from a cylinder to a prism with elliptical cross-section, the set of Bessel functions splits into two sets of radial eigenfunctions, the Mathieu *odd* and *even* functions [9]. As a result, the cutoff frequencies for modes propagating in a waveguide with elliptical cross-section also split, since they are related to the (splitted) roots of Mathieu functions. Adjusting the cutoff frequencies and therefore the phase velocities of the $TE_{11}^{o,e}$ modes (o=odd, e=even, with electric field along major and minor axis of the ellipse respectively), it is possible to make the phase shift ϕ almost independent of frequency.

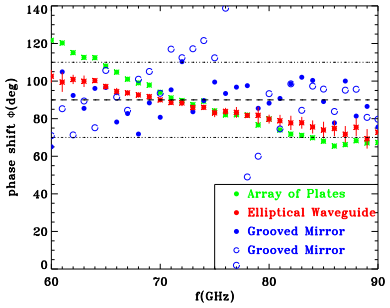

Figure 2: (colour) comparison of phase shifters

In principle a combination of two 45^0 shifters with opposite behaviour (ϕ rising and decreasing with f), for example a "cascade" of a grooved mirror and an array of plates, could also be better. Nevertheless it has been unnecessary, since the elliptical waveguide more than satisfies the diagnostic requirements, as shown in fig.2, and has been adopted. Its linearly polarized output is brought by a transmission line to the same 24 channel heterodyne radiometer employed in ECE measurements at the first harmonic, O-mode [10].

In the past, to let the electron Bernstein emission (EBE) spectrum fall in the frequency range $f = 63 \div 78 GHz$ spanned by the ECE radiometer, the magnetic field had to be lowered to $B = 2.4T$ [2]. The expected Doppler shift for the new sightline is low enough that the computed EBE spectrum (fig.3) matches the band of the radiometer also for routine magnetic field $B = 2.5T$. No new higher frequency local oscillator is therefore required. Modifications will concern only the intermediate frequency section of the radiometer, whose channels are of course optimized for ECE spectra: 8 new channels will be added to improve the resolution where needed by EBE (see fig.3).

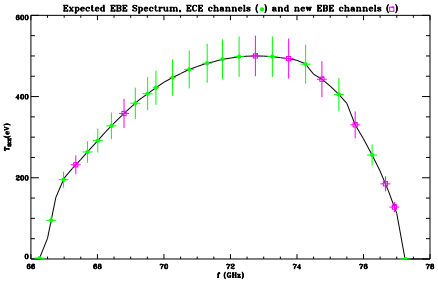

Figure 3: computed EBE spectrum and new channels of the radiometer

Preliminary measurements

Apart from the modifications to the radiometer, the diagnostic is finished and already

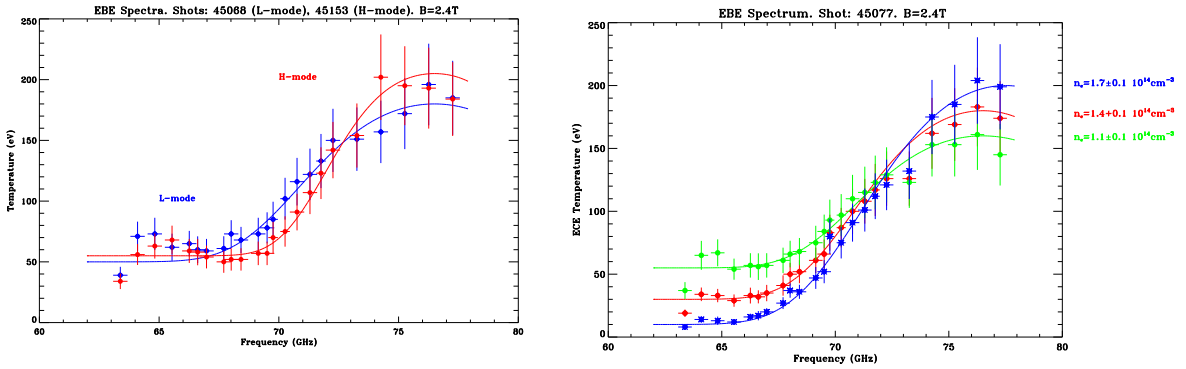

Figure 4: Spectral measurements during a) L and H-mode, b) density ramp

calibrated by the well known hot/cold technique [10]. First results are waited for the next W7-AS campaign, starting in July 2000. Here we present new measurements performed with the temporary set-up described in [2], using an ECRH antenna as receiving antenna viewing along the non-optimized sightline.
As expected, the spectra become steeper during the H-mode (fig.4a).
The pedestal in the spectra can be interpreted in terms of stray radiation, as fig.4b shows. Assuming the form of the density profile to be constant, a density ramp coincides with a ramp of the density-gradient, and, as a result, with an increase of the transmittivity at the cutoff [4]:

$$T = exp\left\{-\pi c L\sqrt{\frac{\omega_{ce}}{2\omega^3}}\ \left[2(1+\frac{\omega_{ce}}{\omega})(k_{\|,opt}-k_{\|})^2+k_y^2\right]\right\}\ ,$$

where $L = n_e/(\partial n_e/\partial x)$ is the density scale length. Simultaneously, the reflectivity at the cutoff layer has to decrease. Results in fig.4b agree with this interpretation: during the density ramp the high frequency part of the spectrum, mainly *transmitted* signal, rises, and the low frequency part, mainly *reflected* stray radiation, falls.

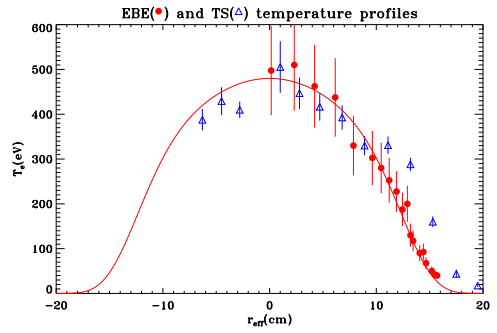

Figure 5: T_e profiles: EBE (red,circles) and Thomson Scattering(blue,triangles)

Ultimately, we have considered the last spectrum available during the density ramp, characterized by the best signal-to-noise ratio. The spectrum has been rescaled to take into account the XO conversion efficiency and the polarization losses, since the elliptical waveguide was not yet installed. By means of the above mentioned ray-tracing code we are now able to convert the spectra in profiles. To our knowledge, the one in fig.5 is the first electron temperature profile measured by EBE. Satisfactory agreement is found with the YAG laser Thomson scattering results. With the new antenna also the high field side of the profile will be available.

Fruitful discussions with W.Kasparek (IPF,Stuttgart) and H.J.Hartfuß (IPP,Garching) are gratefully acknowledged.

References

[1] H.P.Laqua *et al.*, Phys.Rev.Lett.**78**, 3467 (1997)
[2] H.P.Laqua, H.J.Hartfuß and the W7-AS Team, Phys.Rev.Lett.**81**, 2060 (1998)
[3] J.Preinhaelter and V.Kopecký, J.Plasma Phys.**10**, 1 (1973)
[4] E.Mjølhus, J.Plasma Phys.**31**, 7 (1984)
[5] F.R.Hansen, J.P.Lynov and P.Michelsen, Plasma Phys.Control.Fusion **27**, 1077 (1985)
[6] C.B.Forest *et al.*, Phys.Plasmas **7**, 1352 (2000)
[7] S.A.Schelkunoff and H.T.Friis, *Antennas - Theory and Practice*, Wiley 1952
[8] P.F.Goldsmith, *Quasioptical Systems*, IEEE Press, Piscataway(NJ) 1998
[9] M.Abramowitz and I.A.Stegun *Handbook of Math.Functions*, Dover 1974
[10] H.J.Hartfuß *et al., Proc.6th Joint Workshop on ECE and ECRH*, Oxford 1987, p.281; see also H.J.Hartfuß *et al.* Plasma Phys.Control.Fusion **39**, 1693 (1997)